Available online at www.sciencedirect.com
ScienceDirect
Earth and Planetary Science Letters 250 (2006) 486–500
EPSL
www.elsevier.com/locate/epsl

Fe isotope fractionation in iron meteorites: New insights into metal-sulphide segregation and planetary accretion

H.M. Williams [a,b,*], A. Markowski [a], G. Quitté [a], A.N. Halliday [a,b], N. Teutsch [a], S. Levasseur [a]

[a] *Department of Earth Sciences, ETH-Zürich, Sonneggstrasse 5, CH-8092 Zürich, Switzerland*
[b] *Department of Earth Sciences, University of Oxford, Parks Road, Oxford, OX1 3PR, United Kingdom*

Received 19 December 2005; received in revised form 15 August 2006; accepted 16 August 2006
Available online 25 September 2006
Editor: S. King

Abstract

Magmatic iron meteorites are considered to be remnants of the metallic cores of differentiated asteroids, and may be used as analogues of planetary core formation. The Fe isotope compositions ($\delta^{57/54}$Fe) of metal fractions separated from magmatic and non-magmatic iron meteorites span a total range of 0.39‰, with the $\delta^{57/54}$Fe values of metal fractions separated from the IIAB irons ($\delta^{57/54}$Fe 0.12 to 0.32‰) being significantly heavier than those from the IIIAB ($\delta^{57/54}$Fe 0.01 to 0.15‰), IVA ($\delta^{57/54}$Fe −0.07 to 0.17‰) and IVB groups ($\delta^{57/54}$Fe 0.06 to 0.14‰). The $\delta^{57/54}$Fe values of troilites (FeS) separated from magmatic and non-magmatic irons range from −0.60 to −0.12‰, and are isotopically lighter than coexisting metal phases. No systematic relationships exist between metal-sulphide fractionation factor ($\Delta^{57/54}Fe_{M\text{-}FeS} = \delta^{57/54}Fe_{metal} - \delta^{57/54}Fe_{FeS}$) metal composition or meteorite group, however the greatest $\Delta^{57/54}Fe_{M\text{-}FeS}$ values recorded for each group are strikingly similar: 0.79, 0.63, 0.76 and 0.74‰ for the IIAB, IIIAB, IAB and IIICD irons, respectively. $\Delta^{57/54}Fe_{M\text{-}FeS}$ values display a positive correlation with kamacite bandwidth, i.e. the most slowly-cooled meteorites, which should be closest to diffusive equilibrium, have the greatest $\Delta^{57/54}Fe_{M\text{-}FeS}$ values. These observations provide suggestive evidence that Fe isotopic fractionation between metal and troilite is dominated by equilibrium processes and that the maximum $\Delta^{57/54}Fe_{M\text{-}FeS}$ value recorded (0.79 ± 0.09‰) is the best estimate of the equilibrium metal-sulphide Fe isotope fractionation factor. Mass balance models using this fractionation factor in conjunction with metal $\delta^{57/54}$Fe values and published Fe isotope data for pallasites can explain the relatively heavy $\delta^{57/54}$Fe values of IIAB metals as a function of large amounts of S in the core of the IIAB parent body, in agreement with published experimental work. However, sequestering of isotopically light Fe into the S-bearing parts of planetary cores cannot explain published differences in the average $\delta^{57/54}$Fe values of mafic rocks and meteorites derived from the Earth, Moon and Mars and 4-Vesta. The heavy $\delta^{57/54}$Fe value of the Earth's mantle relative to that of Mars and 4-Vesta may reflect isotopic fractionation due to disproportionation of ferrous iron present in the proto-Earth mantle into isotopically heavy ferric iron hosted in perovskite, which is released into the magma ocean, and isotopically light native iron, which partitions into the core. This process cannot take place at significant levels on smaller planets, such as Mars, as perovskite is only stable at pressures >23 GPa. Interestingly, the average $\delta^{57/54}$Fe values of mafic terrestrial and lunar samples are very similar if the High-Ti mare basalts are

* Corresponding author. Department of Earth Sciences, University of Oxford, Parks Road, Oxford, OX1 3PR, United Kingdom. Tel.: +44 1865 282 149; fax: +44 1865 272 072.
E-mail address: helenw@earth.ox.ac.uk (H.M. Williams).

doi:10.1016/j.epsl.2006.08.013

excluded from the latter. If the Moon's mantle is largely derived from the impactor planet then the isotopically heavy signature of the Moon's mantle requires that the impacting planet also had a mantle with a $\delta^{57/54}$Fe value heavier than that of Mars or 4-Vesta, which then implies that the impactor planet must have been greater in size than Mars.

Keywords: Iron isotopes; Iron meteorites; Core formation; Giant impact; Moon; Mars

1. Introduction

Core formation is a critical facet of the earliest history of terrestrial planets, planetary embryos and planetesimals. The abundance and nature of light elements in the core is controversial and bears on planetary bulk compositions, differentiation, core rheology and core–mantle interaction. Sulphur is believed to be a significant light element in the cores of iron meteorite parent bodies and the terrestrial planets, although its exact abundance remains unknown. In this study we present Fe isotope data for metals and sulphides from iron meteorites and use these to investigate core formation processes in the terrestrial planets.

Magmatic iron meteorites are considered to be remnants of the metallic cores of differentiated asteroid-sized parent bodies, and are classed into groups according to variations in their major and trace element concentrations. Non-magmatic iron meteorites (groups IAB and IIICD) are thought to be the products of crystal segregation and fractional crystallisation processes taking place in cooling metallic melts formed by impact heating of chondritic parent bodies [1]. S is present in all iron meteorite groups, usually in the form of discrete FeS (troilite) nodules. S has a low solubility in metal, and would have been progressively excluded from the crystallising metal during cooling of the parent body core, leading to enrichment in the residual metallic melt [2]. Hence troilite nodules within magmatic iron meteorites are commonly interpreted to represent trapped droplets of residual melt [2].

Recent studies have found evidence that high temperature processes such as partial melting can cause detectable Fe isotope fractionations in terrestrial igneous rocks [3–7] and have demonstrated significant Fe isotope variations between olivine, troilite (FeS), kamacite and taenite in pallasite meteorites [4,7,8]. Such Fe isotopic fractionations are of interest because by measuring silicates one may be able to infer the nature of hidden core material. However, isotopic fractionations can be complex and result from either kinetic or equilibrium fractionation processes. Kinetic stable isotope fractionation can occur in situations where there is effectively unidirectional movement of the element of interest, where reaction or transport rates are greater for the lighter isotopes. Processes that can induce kinetic isotope fractionation include diffusion, evaporation and condensation. Equilibrium stable isotope fractionation will take place if there is a change in the binding environment of the element of interest, i.e. in the oxidation or coordination state of Fe or in the nature of the species to which it is bound [9,10]. Isotopic fractionations resulting from equilibrium processes can also be moderated by kinetic fractionation and vice versa. We present Fe isotope data for the separated metal and troilite fractions of 35 iron meteorites, and conclude that the Fe isotope fractionation observed between bulk metal and sulphide is dominantly the product of equilibrium processes, and that, in conjunction with published data from pallasite meteorites [4,7,8], it can be applied to problems of planetary core formation.

2. Analytical techniques

Etched and polished slabs of iron meteorite were sawn using diamond-tipped dentist tools in ethanol. Metal and sulphide fragments were generally sawn within 5 cm of each other, avoiding any obvious sulphide inclusions or carbon-rich schreibersite rims, which commonly surround sulphide inclusions. Metal fragments >30 mg were sawn and if present, fusion crust material or rust on the surface of the metal fragments was removed by polishing the piece with a small diamond saw blade. Sulphide fragments were sawn from the cores of discrete troilite nodules that were ~4–10 mm in diameter. Troilites from Gibeon and North Chile were unusual in that they were extremely small (<3 mm^3) and were not rimmed by schreibersite. In Watson, silicates were manifested as elongate (~0.8 mm × 2 mm) opaque dark green-grey euhedral grains in small oriented clusters, with interconnecting dark rims (<0.2 mm), presumably schreibersite. The silicates were located <0.5 mm from the fusion crust of the meteorite chip obtained. Care was taken to ensure that schreibersite and fusion crust material was removed from the silicates prior to their dissolution by picking them under ethanol in a binocular microscope. Replicate

Table 1
Iron isotope results from iron meteorites: metal fractions

Sample	Group	Kamacite bandwidth (mm)	$\delta^{57/54}$Fe	2 S.D.	$\delta^{56/54}$Fe	2 S.D.	*n*
Murphy*	IIA	n/a	0.12	0.05	0.11	0.14	6
Coahuila 1*	IIA	n/a	0.17	0.08	0.01	0.15	3
Coahuila 2*	IIA	n/a	0.22	0.10	0.15	0.33	6
Bennett County*	IIA	n/a	0.17	0.10	0.10	0.09	10
Negrillos*	IIA	n/a	0.18	0.10	0.09	0.13	8
North Chile	IIA	n/a	0.23	0.03	0.22	0.08	6
Gressk 1	IIA	n/a	0.28	0.07	0.18	0.07	7
Gressk 2	IIA	n/a	0.31	0.11	0.29	0.22	6
Guadalupe y Calvo*	IIA	n/a	0.32	0.09	0.21	0.10	8
Navajo*	IIB	10.0	0.13	0.10	0.01	0.13	3
Sao Juliao de Moreira*	IIB	6.0	0.19	0.03	0.05	0.08	4
Sikhote Alin*	IIB	9.0	0.19	0.07	0.08	0.12	8
Mount Joy*	IIB	10.0	0.22	0.13	0.09	0.10	8 (5)
Merceditas 1	IIIA	1.0	0.04	0.11	0.02	0.16	9
Merceditas 2	IIIA	1.0	0.01	0.08	0.02	0.12	3
Mount Edith*	IIIB	0.8	0.04	0.09	0.02	0.13	6
Grant*	IIIB	0.8	0.13	0.09	0.14	0.15	4
Chupaderos*	IIIB	0.7	0.14	0.07	0.05	0.09	2
Bear Creek	IIIB	0.6	0.15	0.08	0.16	0.18	5
Gibeon	IVA	0.30	−0.07	0.02	−0.08	0.12	4
Duchesne	IVA	0.30	−0.05	0.13	−0.1	0.20	11
Bushman Land*	IVA	0.33	0.02	0.08	−0.01	0.27	6
Duel Hill*	IVA	0.30	0.16	0.06	0.12	0.12	3
Yanhuitlan	IVA	0.30	0.17	0.06	0.11	0.14	8 (7)
Tawallah Valley	IVB	0.01	0.06	0.12	0.04	0.20	10
Chinga*	IVB	0.01	0.08	0.01	−0.06	0.02	2
Warburton Range*	IVB	0.01	0.11	0.10	0.04	0.09	8
Tlacotepec 1*	IVB	0.03	0.15	0.09	0.09	0.36	6
Tlacotepec 2 (fusion crust)*	IVB	0.03	0.14	0.09	−0.03	0.14	6
Arispe*	IC	2.9	0.18	0.09	0.12	0.18	6
Carbo 1*	IID	0.90	0.13	0.01	−0.04	0.12	2
Carbo 2*	IID	0.90	0.14	0.03	0.02	–	2 (1)
Carbo 3*	IID	0.90	0.21	0.09	0.13	0.13	6
Hraschina*	IID	0.70	0.27	0.05	0.20	0.26	7
Watson	IIE	n.d.	0.01	0.09	−0.05	0.17	4
Clark County*	IIIF	1.0	0.14	0.03	0.07	0.18	2
Nelson County*	IIIF	5.0	0.17	0.01	0.00	0.03	2
Seeläsgen	IIICD	3.1	0.16	0.11	0.10	0.10	5
Mundrabilla 1*	IIICD	0.60	0.20	0.08	0.15	0.23	6
Mundrabilla 2*	IIICD	0.60	0.18	0.10	0.15	0.15	4
Canyon Diablo*	IAB	2.0	0.12	0.07	0.01	0.09	4
Odessa	IAB	1.7	0.13	0.07	0.12	0.08	6
Toluca 1*	IAB	1.7	0.20	0.04	0.16	0.03	4
Toluca 2*	IAB	1.7	0.20	0.02	0.11	0.11	3
Caddo County*	IAB	n.d.	0.24	0.05	0.23	0.13	5

Iron isotope data for the metallic fractions (combined kamacite and taenite phases) for magmatic and non-magmatic iron meteorites. Asterisks indicate that the samples were obtained as aliquots of dissolutions prepared for other studies [11–13]; n/a indicates a measurement that is not applicable to the sample(s) listed, in this case kamacite bandwidths cannot be determined for the IIA hexahedrites as their metal phase consist of almost pure kamacite; n.d., indicates not determined. Errors are 2 S.D., based on replicate analyses of the dissolutions (*n*=number of replicates, bracketed values are for $\delta^{57/56}$Fe, as more scatter was observed in these measurements and some individual measurements had to be excluded). Tlacotepec 2 (fusion crust) is a metal fragment from which the fusion crust could not be completely removed.

metal dissolutions were carried out for a number of samples in order to evaluate the effects of differential taenite–kamacite sampling and Fe isotope heterogeneity (Table 1). Replicate dissolutions of sulphide fragments were also undertaken for several meteorites (Table 2). Procedural blanks for sawing were estimated by sawing ultra-pure synthetic quartz prior to dissolving it in HF-HNO_3 and HCl and comparing the Fe abundances of sawn and pristine quartz dissolutions. Sawing blanks were <20 ng, negligible compared to sample sizes, which were >500 μg Fe. A number of samples were also obtained as aliquots from much larger dissolutions (70 mg–2 g) prepared for W, Ag and Tl isotope analyses [11–13], including troilites from Mundrabilla, Toluca and Canyon Diablo.

Sample dissolution and iron extraction procedures followed methods described previously [5,6]; additional details applicable to this work are detailed below. All samples were treated with aqua regia and, following evaporation, were then refluxed with H_2O_2 and HNO_3, which were subsequently evaporated. Silicates were treated with ~10:1 concentrated HF:HNO_3 following this step. For all samples, these dissolution stages were followed by 2 reflux and evaporation cycles of 6M HCl at 190 °C. Fe was purified using anion exchange chromatography in HCl form, and the Fe column cuts obtained were treated with H_2O_2 and HNO_3. Following a final evaporation, the samples were dissolved in 0.05M HCl for mass spectrometry. Total procedural blanks were <10 ng. As documented previously [6], Fe yields were quantitative and no measurable Fe isotope fractionation took place on the columns following these procedures. To assess matrix effects, the pure Fe standard IRMM-14

Table 2
Iron isotope results from iron meteorites: troilite and silicates

Sample	Class	$\delta^{57/54}$Fe	2 S.D.	$\delta^{56/54}$Fe	2 S.D.	*n*
North Chile sulphide 1	IIA	−0.56	0.09	−0.43	0.11	6
North Chile sulphide 2	IIA	−0.47	0.12	−0.34	0.18	9
North Chile sulphide 3	IIA	−0.46	0.10	−0.33	0.14	7
Gressk sulphide	IIA	0.01	0.12	−0.02	0.18	
Merceditas sulphide 1	IIIA	−0.60	0.07	−0.40	0.18	6
Merceditas sulphide 2	IIIA	−0.59	0.05	−0.45	0.03	3
Grant sulphide	IIIB	−0.18	0.12	−0.10	0.18	2
Bear Creek sulphide	IIIB	0.01	0.07	−0.04	0.17	10
Gibeon sulphide	IVA	−0.12	0.05	−0.10	0.21	9
Watson silicate 1	IIE	−0.06	0.10	−0.08	0.14	4
Watson silicate 2	IIE	−0.05	0.04	−0.12	0.16	3
Seelägsen sulphide 1	IIICD	−0.58	0.08	−0.36	0.13	3
Seelägsen sulphide 2	IIICD	−0.55	0.12	−0.41	0.02	5
Mundrabilla sulphide*	IIICD	−0.40	0.06	−0.28	0.09	6
Canyon Diablo sulphide 1*	IAB	−0.41	0.08	−0.32	0.06	8
Canyon Diablo sulphide 2*	IAB	−0.21	0.02	−0.15	0.01	3
Odessa sulphide	IAB	−0.25	0.09	−0.20	0.22	4
Toluca sulphide*	IAB	−0.56	0.09	−0.37	0.10	5

Iron isotope data for the non-metallic fractions (troilites and a silicate phase from Watson) for magmatic and non-magmatic iron meteorites. Asterisks indicate that the samples were obtained as aliquots of dissolutions prepared for other studies. Errors and replicates as in Table 1.

was added to the eluted matrix fractions of several samples (metals: Mundrabilla, Canyon Diablo, Bushman Land; sulphides: Merceditas, Canyon Diablo, Toluca) in quantities matching the original amounts of Fe in the samples, and these mixtures were then processed through columns and analysed for their isotopic abundance. The resultant $\delta^{57/54}$Fe values, where the δ notation is used to express the per mil deviation of the measured ratio relative to a standard e.g. $\delta^{57/54}Fe = (^{57}Fe/^{54}Fe_{sample}/^{57}Fe/^{54}Fe_{IRMM\text{-}14} - 1) * 10^3$ were: Mundrabilla metal: 0.11±0.06‰; Canyon Diablo metal: −0.01±0.05‰; Bushman Land metal: −0.05±0.04‰; Merceditas sulphide: −0.03±0.13‰; Canyon Diablo sulphide: 0.09±0.05‰; Toluca sulphide: 0.02±0.12‰ (errors are 2 S.D.). When evaluated relative to our long-term reproducibility for $\delta^{57/54}$Fe (0.10‰, 2 S.D.) it is clear that there are no resolvable matrix effects. To evaluate the effect of S on iron purification, we added pure native S, dissolved in aqua regia, to IRMM-14 in 1:1 M quantities of Fe and S, and treated this mixture as an unknown through our dissolution and chemical purification procedure. The $\delta^{57/54}$Fe value of this mixture was 0.06±0.02‰, which, relative to the long-term reproducibility, demonstrates that there are no matrix effects specifically associated with sulphides.

Iron isotope analyses were carried out on a standard-resolution ($M/\Delta M \sim 400$) Nu Instruments (Wrexham, UK) multi-collector inductively coupled mass spectrometer (MC-ICPMS) and follow established protocols [6], with the exception that ^{56}Fe was collected in a Faraday bucket (H4) with $10^9\Omega$ resistor rather than a $10^{10}\Omega$ resistor (L5). This change in routine allows the ^{56}Fe/^{54}Fe ratio to be directly measured in a single cycle; in previous studies [6], the position of the $10^{10}\Omega$ resistor on L5 and the positions of the three ion counters (a consequence of other instrument applications) required two integration cycles in order to collect 56 in L5 and cover the mass range of 53 to 57. Iron concentrations of the solutions analysed were 8–10 ppm, giving rise to beams $4–9\times10^{-10}$A in size. Interferences from ^{54}Cr (monitored with ^{53}Cr and ^{52}Cr), ArN^+ and ArO^+ are the same as those documented previously [6]. The long-term reproducibility for the modified collection routine was determined by repeat analysis of the ETH internal hematite standard which gave mean $\delta^{57/54}$Fe and $\delta^{56/54}$Fe values of 0.82±0.10‰ and 0.58±0.18‰, respectively (2S.D.; n=136). These values are in excellent agreement with those previously obtained for this standard in the ETH laboratory and elsewhere [6].

3. Results

The Fe isotope compositions ($\delta^{57/54}$Fe) of metal fractions (Table 1, Fig. 1) separated from magmatic and non-magmatic iron meteorites span a range of 0.39‰. Duplicate metal dissolutions have $\delta^{57/54}$Fe values differing from each other by <0.08‰, insignificant relative to the long-term $\delta^{57/54}$Fe reproducibility of 0.10‰. The $\delta^{57/54}$Fe values of metal fractions that were leached prior to dissolution are not significantly (Student's *t*-test, 95% confidence) different to those that were not. Metal fractions separated from the IIAB, IIIAB, IVA and IVB irons have $\delta^{57/54}$Fe values ranging from 0.12 to 0.32‰, 0.01 to 0.15‰, −0.07 to 0.17‰ and 0.06 to 0.14‰, respectively. Metal fractions from the non-magmatic IAB and IIICD groups have $\delta^{57/54}$Fe values ranging from 0.12 to 0.24‰, and 0.16 to 0.20‰, respectively. Student's *t*-tests indicate that the average $\delta^{57/54}$Fe values of IIA and IIB metals are not distinguishable, but that the combined average $\delta^{57/54}$Fe value of the IIAB metals is significantly heavier than the average $\delta^{57/54}$Fe values of the IIIAB, IVA and IVB metals at the 95% confidence level. The average $\delta^{57/54}$Fe values of all the other groups, magmatic and non-magmatic, are statistically indistinguishable.

Troilites have lighter $\delta^{57/54}$Fe values than the coexisting metal fractions (Table 2, Fig. 1). Replicate

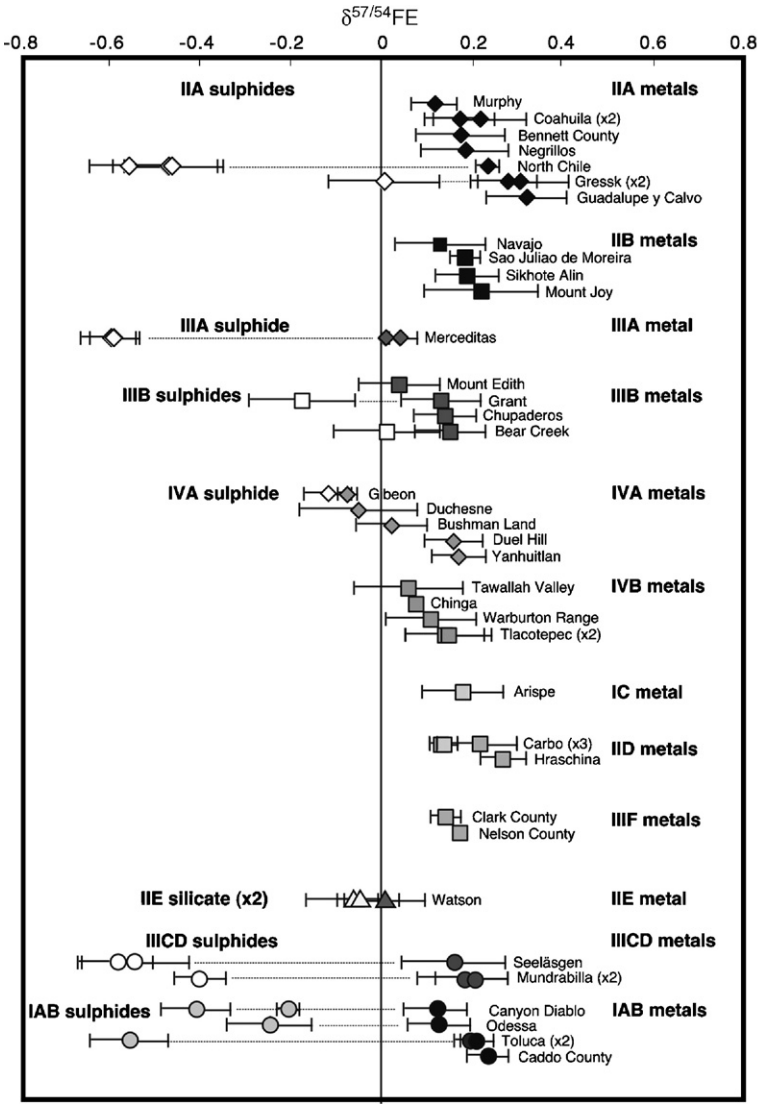

Fig. 1. Fe isotope data for the metal and troilite fractions of iron meteorites. Error bars are 2 S.D., based on replicate analyses, and are given for metals in Table 1 and for non-metallic phases in Table 2.

troilite dissolutions have $\delta^{57/54}$Fe values that are generally within 0.10‰ of each other, although troilites from Canyon Diablo are an exception, differing by 0.20‰. This could be caused by contamination of the troilite fraction with metal, as the latter has a heavier isotopic composition, or could represent a genuine isotopic heterogeneity. The direction of the fractionation between troilite and metal reported here is in agreement with Fe isotope data for pallasites reported by Weyer et al. [4], although our data extends to larger metal–troilite fractionation factors. However, the direction is the opposite of that reported by Poitrasson et al. [8] in pallasites. The $\delta^{57/54}$Fe values of troilites range from −0.60 to −0.12‰, and do not appear to be related to iron meteorite group and age or to bulk sample elemental concentrations or ratios that are indicative of fractional crystallisation processes. Also, there are no correlations of either troilite $\delta^{57/54}$Fe values or calculated metal–troilite fractionation factors ($\delta^{57/54}Fe_{metal} - \delta^{57/54}Fe_{FeS}$; $\Delta^{57/54}Fe_{M\text{-}FeS}$) with recently reported apparent Ni isotopic anomalies (ε^{60}Ni and ε^{61}Ni) in the troilites [14], although there is a hint that the samples with the greatest $\Delta^{57/54}Fe_{M\text{-}FeS}$ values have larger ε^{60}Ni and ε^{61}Ni anomalies. Troilite $\delta^{57/54}$Fe and $\Delta^{57/54}Fe_{M\text{-}FeS}$ values do however correlate with kamacite bandwidth [15] (Fig. 2).

Only one silicate-metal pair was analysed, from the IIE iron Watson. Duplicate silicate dissolutions agreed

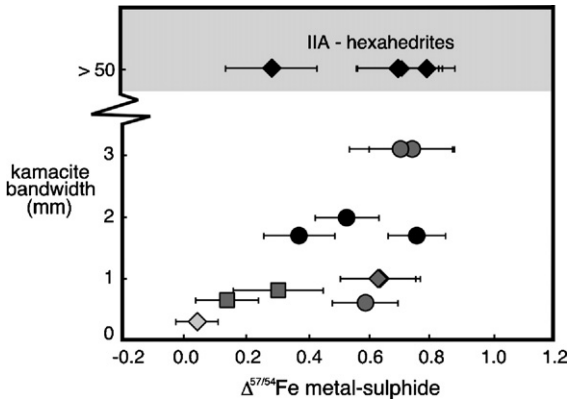

Fig. 2. A) Metal-sulphide fractionation factors ($\Delta^{57/54}Fe_{M\text{-}FeS}$) plotted against kamacite bandwidth [15]. The IIA hexahedrites are plotted at the arbitrary bandwidth of >50 mm as their metallic structure is too coarse for the determination of meaningful bandwidths. Symbols are different for each group of meteorites and follow those used in Fig. 1.

to within 0.01‰. The resulting metal-silicate fractionation factor for Watson ($\delta^{57/54}Fe_{metal} - \delta^{57/54}Fe_{silicate}$; $\Delta^{57/54}Fe_{M\text{-}Sil}$) is 0.07±0.14‰, overlapping the lower end of the range of $\Delta^{57/54}Fe_{M\text{-}Sil}$ values determined in pallasites [4,7,8].

4. Discussion

4.1. Iron isotope fractionation between troilite and metal — kinetic or equilibrium?

The variations in troilite $\delta^{57/54}$Fe and $\Delta^{57/54}Fe_{M\text{-}FeS}$ values could reflect stable isotope fractionation between these phases, or could indicate that metal and troilite have different origins and have not equilibrated. Recent studies on the same iron meteorites [14] have demonstrated that resolvable non-mass dependent ε^{60}Ni and ε^{61}Ni anomalies appear to be present in troilites, but not in the metal, which could indicate different origins. The preferred explanation for the ε^{60}Ni and ε^{61}Ni anomalies is that they result from the admixing of pre-solar grains containing exotic Ni into the iron meteorite parent bodies and that this exotic Ni component is most apparent in troilites, which have lower initial Ni contents relative to the metal [14]. Substantial heterogeneity exists in the ε^{60}Ni (spanning 1.6 and 2.2 ε for Odessa and Toluca, respectively) and ε^{61}Ni (spanning 8.6 and 12.0 ε for Odessa and Toluca, respectively) values of individual troilites from the same meteorites relative to the entire isotopic variation observed in magmatic and non-magmatic irons (4.2 and 18.0 ε, for ε^{60}Ni and ε^{61}Ni respectively) whereas minimal heterogeneity exists for Fe isotopes, providing evidence that different processes control nucleosynthetic Ni and stable Fe isotope systematics in iron meteorites.

Fe isotopic fractionation between metal and troilite may have been produced by either kinetic or equilibrium fractionation processes, or a combination of both. We can investigate whether or not the range observed in $\Delta^{57/54}Fe_{M\text{-}FeS}$ values, from 0.04 (Gibeon, IVA) to 0.79‰ (North Chile, IIA) can be produced by purely kinetic processes using mass balance calculations. Kinetic fractionation could take place during processes such as initial sulphide exsolution at the Fe–FeS eutectic (~990 °C [16]) where iron is transferred from the metal phase to the forming sulphide or subsolidus diffusive exchange between metal and sulphide during cooling, at temperatures ranging from the Fe–FeS eutectic to below effective blocking temperatures for iron (~500 °C [17]). Later events such as impact-related volatilisation and melting may also be applicable in limited cases. In the models below, we consider kinetic fractionation during subsolidus diffusion only. The magnitude of kinetic isotope fractionation during initial sulphide nucleation should be much smaller than any kinetic fractionation associated with subsolidus diffusion, which takes place at lower temperatures where differences in the diffusion rates of heavy and light isotopes are enhanced.

It is assumed that $\Delta^{57/54}Fe_{x-y} \sim 1000\ln\alpha$, where $\alpha = (mass_{57}/mass_{54})^{\beta}$. β is generally assumed to have a value of 0.1 for diffusion in melts [18], although β values determined for Fe in silicate melts range from 0.075 [19] to 0.27 [20]. For β values of 0.1, 0.2 and 0.3, $1000\ln\alpha$ values are −5.4, −12.2 and −16.8, respectively. For Fe diffusion from the metallic melt to the exsolving sulphide we assume that the metallic melt provides an infinite reservoir for Fe. Taking the most fractionated sample, North Chile, as an example, we calculate how much kinetically fractionated Fe must be introduced into a sulphide, where both metal and sulphide have initial $\delta^{57/54}$Fe values of 0‰, to obtain a final $\delta^{57/54}$Fe value of −0.79‰:

$$\delta^{57/54}Fe_{FeS,meas} = f_{ini} * \delta^{57/54}Fe_{FeS,ini} + f' * 1000\ln\alpha \quad (1)$$

Where $\delta^{57/54}Fe_{FeS,meas}$ is the final measured, isotopic composition of the sulphide and takes a value of −0.79, f_{ini} is the number of moles of unfractionated Fe initially present in the troilite, $\delta^{57/54}Fe_{FeS,ini}$ is the isotope composition of that initial Fe and takes a value of 0, f' is the number of moles of kinetically fractionated iron diffused from the metal into the troilite (the sum of f_{ini} and f' equals the final molar amount of iron in the sample) and $1000\ln\alpha$ takes different values according to

β. The calculation is carried out using absolute isotope ratios which are ultimately converted into the delta notation. Using β values of 0.1, 0.2 and 0.3, the relative proportions of kinetically fractionated iron that must be diffused into the troilite (f') are 0.15, 0.07 and 0.05, respectively, corresponding to 9.3, 4.6 and 3.1 wt.% of the sulphide assuming a 1:1 M ratio for Fe and S in troilite. However, during subsolidus diffusion it is impossible to diffuse Fe into troilite without diffusing another metal cation from the troilite to the metal in equivalent molar proportions. This co-diffusing metal must be Ni, as it is the only other metal of sufficient abundance in iron meteorites to exchange with Fe; moreover it is more siderophile than Fe. The initial amount of Ni in the troilite is the sum of the moles of Ni lost (equal to f', the moles of Fe added) and the current number of moles of Ni present in the troilite. The latter is calculated from the measured Fe/Ni ratio of North Chile troilites (1560, [14]) and assuming that the molar ratio of (Fe,Ni) to S is 1:1 in troilite and that troilites only consist of Fe, Ni and S. For β values of 0.1, 0.2 and 0.3, the proportions of nickel atoms lost from the sulphide relative to the initial amount of nickel are 0.9978, 0.9956 and 0.9935. In contrast to the metal phase, troilites form a very limited, finite reservoir for Ni, due to their low Ni abundances and relative rarity in iron meteorites. For illustrative purposes, we can calculate the maximum theoretical amount of Ni isotopic fractionation that must accompany the removal of such large amounts of Ni assuming that the loss of Ni from troilite to metal follows Rayleigh distillation. This is an extreme-end member process that fractionates isotopes in the most efficient way; it describes the exponential enrichment or depletion of an isotope that occurs in the residual reservoir of the reactant as it is converted into a product. In this model isotopic fractionation is driven by the mass dependent transfer of the element of interest from one reservoir to another and the actual mechanism of transfer, e.g. volume diffusion, is not defined. By using this model we are assuming that the loss of Ni from the troilite reservoir produces the most isotopic fractionation, and that any effects resulting from diffusion-induced fractionation are minor in comparison.

$$\delta^{62/58}\mathrm{Ni}_{\mathrm{FeS,meas}} = \delta^{62/58}\mathrm{Ni}_{\mathrm{FeS,ini}} * (1-f')^{(\alpha-1)} \quad (2)$$

In Eq. (2), $\delta^{62/58}\mathrm{Ni}_{\mathrm{FeS,ini}}$ and $\delta^{62/58}\mathrm{Ni}_{\mathrm{FeS,meas}}$ are the Ni isotope compositions of the initial and measured Ni components, α is the fractionation factor and f' is the amount of kinetically removed Ni. The actual isotopic composition of the initial Ni present does not affect the calculation; here we use a value of 0 so that we can evaluate the *relative* change in nickel isotopic composition as a function of kinetic fractionation during diffusion. For β values of 0.1, 0.2 and 0.3, we obtain theoretical $\delta^{62/58}\mathrm{Ni}_{\mathrm{FeS,meas}}$ values of +41.5, +74.6 and +104.7‰, compared to actual measured $\delta^{62/58}$Ni values for troilites which range from −4.96 to +3.03‰ [21]. Although the theoretical $\delta^{62/58}\mathrm{Ni}_{\mathrm{FeS,meas}}$ values are only a first-order upper limit on the amount of isotopic fractionation possible, they suggest that pure kinetic fractionation is an unlikely means of generating the Fe isotope signatures observed. This does not rule out combined equilibrium–kinetic scenarios. If we assume that the Ni isotope variations in troilites are the product of pure kinetic isotope fractionation we can then calculate the molar fraction of Ni that must have been lost from the troilite using Eq. (2), and from this, we can then calculate the magnitude of the Fe kinetic isotope fractionation expected for the amount of Fe that must have been transferred. As above, North Chile troilite, which has a stable $\delta^{62/58}$Ni value of 1.19±0.25‰ [14], is used as an example. For β values of 0.1, 0.2 and 0.3, the molar fractions of Ni lost (and hence of Fe gained) are all below 0.005. Mass balance calculations, following Eq. (1), show that the introduction of such small amounts of kinetically fractionated Fe cannot perturb the initial troilite $\delta^{57/54}$Fe. This calculation demonstrates that while kinetic fractionation may explain $\delta^{62/58}$Ni variations in troilites, mass balance prevents it from being a viable explanation for their Fe isotope compositions.

4.2. Equilibrium stable isotope fractionation between metal and troilite — relationships to meteorite thermal history

As scenarios involving kinetic stable isotope fractionation are unable to explain the isotopic variations observed, equilibrium fractionation, potentially caused by differences in the bonding environments of Fe in metal and troilite or by the contrast in Fe redox state between troilite (Fe^{2+}) and native iron, is the only alternative. However, the range in $\Delta^{57/54}\mathrm{Fe}_{\mathrm{M\text{-}FeS}}$ is puzzling. Possible explanations include kinetic fractionation during initial sulphide nucleation followed by incomplete isotopic equilibrium, dependence of $\Delta^{57/54}\mathrm{Fe}_{\mathrm{M\text{-}FeS}}$ on temperature or on metal and sulphide composition, and late resetting of troilite isotopic systematics, by impact-related volatilisation processes, say. $\Delta^{57/54}\mathrm{Fe}_{\mathrm{M\text{-}FeS}}$ values show a diffuse positive correlation with kamacite bandwidth (Fig. 2). Kamacite bandwidth is a broad indicator of cooling rate, with the

largest bandwidths generally being associated with the slowest cooling rates. Unfortunately, independent cooling rate estimates are not available for all of the meteorites studied here and it is not possible to plot $\Delta^{57/54}Fe_{M\text{-}FeS}$ values against cooling rate directly. In principle, a slower cooling rate should lead to more extensive diffusion, and in the case of unidirectional transport of Fe and kinetic fractionation, this could produce the positive correlation between $\Delta^{57/54}Fe_{M\text{-}FeS}$ values and kamacite bandwidth fractionation. However, unidirectional transport of Fe is only possible during initial sulphide nucleation, and not during subsolidus diffusion, and as discussed above, kinetic fractionation during subsolidus diffusion cannot explain the isotopic variations observed.

Another interpretation of Fig. 2 is that the sulphides initially grew out of isotopic equilibrium and that isotopic equilibrium between metal and sulphide occurred during subsolidus diffusion. In this case, the slowest-cooling meteorites, which generally have the greatest $\Delta^{57/54}Fe_{M\text{-}FeS}$ values, are closest to metal–troilite equilibrium, and that samples with lower $\Delta^{57/54}Fe_{M\text{-}FeS}$ values have not completely equilibrated. Further interpretations of Fig. 2 would be that $\Delta^{57/54}Fe_{M\text{-}FeS}$ is dependent on temperature, metal composition and the amount of S in the meteorites. Temperature dependence is difficult to test without a cogenetic suite of iron meteorites, but experimental data for high temperature Fe isotope fractionation between pyrrhotite ($Fe_{1-x}S$) and synthetic peralkaline rhyolitic silicate melt [22,23] indicates that there is no temperature dependence of the equilibrium fractionation factor (ca −0.45‰ for $\delta^{57/54}Fe$) between the two melts at 840–1000 °C. As yet no data exists for lower temperatures. Temperature dependence could also be reflected in correlations of $\Delta^{57/54}Fe_{M\text{-}FeS}$ values and indices of fractionation such as Ir/Au and Ga/Ge but no such correlations exist. The growth of kamacite–taenite lamellae is influenced by many other factors, such as bulk meteorite Ni and P content, the latter increasing the diffusivity of Ni and influencing kamacite nucleation mechanisms [17]. Therefore any relationships between kamacite bandwidth and $\Delta^{57/54}Fe_{M\text{-}FeS}$ could be a function of metal composition. However, no clear correlations exist between $\Delta^{57/54}Fe_{M\text{-}FeS}$ values and Fe, Ni or P contents. Finally, while the $\Delta^{57/54}Fe_{M\text{-}FeS}$ values could reflect the amount of S present in the meteorite, there are no correlations between $\Delta^{57/54}Fe_{M\text{-}FeS}$ value, S, or any chalcophile elements. Therefore, the array in Fig. 2 is interpreted to be dominantly the product of initial troilite growth out of isotopic equilibrium, followed by variable degrees of isotopic equilibrium during subsolidus diffusion.

The likelihood of metal and troilite being in Fe isotopic equilibrium can be evaluated by calculating the time required for isotopic equilibration for a given length-scale and diffusivity using the relationship $\tau = L^2/D$, where τ = the time period for the return of the system to equilibrium over a lengthscale, L, and D is the diffusivity of Fe at a specified temperature. Isotopic equilibrium must take place in the time interval between initial troilite nucleation (commencing at the Fe–FeS eutectic ~990 °C [16]) and cooling to a temperature below which Fe–Ni inter-diffusion effectively ceases (~500 °C [17]). Experimentally determined Fe–Ni inter-diffusion rates [17] in kamacite and taenite are used for D. For simplicity we do not vary D during cooling. Fe–Ni inter-diffusion is limited by the slower diffusion of Ni, so these diffusion rates are minimum estimates for the diffusion of Fe. Although no inter-diffusion rates are available for troilite, the diffusion rate of Fe in $Fe_{0.8}S$ melt at 840 °C is 1.08×10^{-6} cm^2/s [24] suggests that diffusion rates of Fe and Ni will be much greater in troilite than metal. The values of τ at length-scales applicable to our sampling scale (horizontal distance between metal and the cores of troilite nodule) can be compared with the amount of time that the meteorites were within the "time window" where solid-state Fe–Ni inter-diffusion is possible. The latter is calculated using independent estimates of meteorite cooling rates assuming linear cooling and that troilite segregation begins at 990 °C and that Fe diffusion ceases at 500 °C. The assumption of linear cooling renders all calculated time windows for Fe–Ni inter-diffusion maximum estimates.

Cooling rates for the IIAB irons Quillagua and Tocopilla, believed to be equivalent masses of the North Chile meteorite fall, are 1 and 3 °C/My, respectively [25]. The average rate of 2 °C/My corresponds to a Fe–Ni diffusion time window of 245 My. The IIAB meteorites have bulk P contents of ~0.3 wt.% and consist almost entirely of kamacite. Hence appropriate D values range from 5.5×10^{-16} cm/s (600 °C, kamacite containing 2% Ni and 0.3% P) to 2.8×10^{-12} cm/s (844 °C, kamacite containing 1% Ni and 0.3% P). For a D of 5.5×10^{-16} cm/s and a lengthscale of 0.5 cm, the time required for equilibrium is 14.5 My, for a D of 1.7×10^{-12} cm/s it is 0.03 My, compared to an available time window of 245 My. In order to achieve an equilibration time >245 My, the diffusion rate would have to be $<3.3\times10^{-17}$ cm/s, a value considerably lower than any of the existing estimates [17]. Therefore North Chile is most likely to be in isotopic equilibrium. No cooling rate data are available for the meteorite Gressk, but it is texturally highly shocked, containing

shock-melted troilites [26]. Hence its apparently very low $\Delta^{57/54}Fe_{M\text{-}FeS}$ value may reflect late disruption of Fe isotope systematics — loss of isotopically light Fe due to impact-related volatilisation or melting events could enrich the residual troilite in heavy Fe. Including the non-magmatic irons, the only other iron studied here that is texturally intensely shocked [26] is the IIIB iron Bear Creek, which also has a very low $\Delta^{57/54}Fe_{M\text{-}FeS}$ value.

The IIIAB irons contain ~0.5 wt.% P and have extremely variable cooling rates, ranging from 56 to 338 °C/My with an average of 132 °C/My [27]. For cooling rates of 50, 75, 150 and 400 °C/My, the corresponding Fe diffusion time windows are 10, 6.5, 3.3 and 1.3 My. The diffusion rates used above for the IIAB irons are applicable here, giving equivalent durations for isotopic equilibration (0.03 to 14.5 My). Comparison of these equilibration times with the time windows for diffusive equilibration indicates that the degree of isotopic equilibration attained by IIIAB irons is likely to be highly variable.

Only one IVA metal–troilite pair was studied; Gibeon cooled at 580 °C/Myr [28], and hence had a maximum Fe–Ni inter-diffusion time window of ~0.85 My. Gibeon contains 0.04 wt.% P; Fe–Ni inter-diffusion rates determined for taenite and kamacite with appropriately low P contents range from 1.2×10^{-17} cm/s to 8.3×10^{-15} cm/s. Using an average D of 2.12×10^{-15} cm/s and a length-scale of 0.5 cm, the time-scale required for isotopic equilibration is 3.8 Myr for a closure temperature of 500 °C, implying that metal and troilite in Gibeon are unlikely to be in isotopic equilibrium.

The greatest $\Delta^{57/54}Fe_{M\text{-}FeS}$ values recorded in the IIAB, IIIAB, IAB and IIICD groups are extremely similar: 0.79, 0.63, 0.76 and 0.74‰, respectively. This observation cannot be explained by kinetic processes, strongly suggesting that these fractionation factors approach an equilibrium value. The maximum $\Delta^{57/54}Fe_{M\text{-}FeS}$ values recorded by the non-magmatic irons are essentially the same as the magmatic irons, which would imply that isotopic fractionation records late stage processes, such as subsolidus diffusion and final equilibrium between crystallised metal and sulphide. Although only semi-quantitative, the diffusion calculations above indicate that out of the all iron meteorites studied, North Chile, where $\Delta^{57/54}Fe_{M\text{-}FeS}=0.79$‰, is the most likely to be in isotopic equilibrium. Therefore the fractionation factor between metal and troilite must be at least 0.79‰ (the greatest $\Delta^{57/54}Fe_{M\text{-}FeS}$ value, determined for North Chile), and the range of $\Delta^{57/54}Fe_{M\text{-}FeS}$ values observed in the different meteorite groups probably reflects variable degrees of metal–troilite equilibrium, and potentially late impact-related melting or volatilisation events.

Substantial equilibrium stable isotope fractionation between troilite and metal is broadly consistent with experimental data for Fe isotope fractionation between pyrrhotite ($Fe_{1-x}S$) and synthetic peralkaline rhyolitic silicate melt [22,23], which gives an equilibrium fractionation factor between pyrrhotite and silicate melt of ca −0.45‰ for $\delta^{57/54}Fe$. Data for the iron Watson and for pallasites [4,7,8] provide evidence that silicates are 0.07 to 0.32‰ lighter than coexisting metal phases. Combined, these data provides suggestive evidence of substantial equilibrium metal-sulphide fractionation, which is consistent with new high temperature experimental studies of Fe isotope fractionation between silicate melts and metallic alloys, in which the silicate melt is lighter than the metal by 0.2±0.15‰/amu [20]. If all these observations are taken together, they predict metal-sulphide equilibrium fractionation factors of 0.52 to 1.05‰, consistent with our estimate of 0.79‰.

4.3. Sulphur contents of the parent body cores of magmatic iron meteorites: constraints from Fe isotopes

The general agreement between Fe isotope fractionation factors derived from high temperature experiments and from natural samples suggests that isotopic fractionation factors determined for iron meteorites and pallasites can be applied to the segregation of metallic, sulphide and silicate melts and their subsequent subsolidus equilibrium. The fractionation factors obtained from meteorites are likely to be greater than those applicable to parent body core segregation and crystallisation processes, as the latter take place at higher temperatures and pressures. Nonetheless, they can be used speculatively in mass balance models exploring the metal-sulphide-silicate equilibration during core segregation and the effect that this has on the Fe isotope compositions of planetary cores and mantles. In Eq. (3), we consider a system where the silicate, metal, and sulphide reservoirs of the planet reach isotopic equilibrium simultaneously:

$$\delta^{57/54}Fe_B = \delta^{57/54}Fe_{Sil}{*}f_{Sil} + \delta^{57/54}Fe_M{*}f_M + \delta^{57/54}Fe_{FeS}{*}f_{FeS} \quad (3)$$

In Eq. (3), $\delta^{57/54}Fe_B$ is the bulk composition of the planet and is set to a value of 0 so that relative differences in the Fe isotope compositions of planetary reservoirs can be calculated. This is also consistent with currently available Fe isotope data for chondrites [29–31], where the average $\delta^{57/54}Fe$ value of bulk chondrites

(carbonaceous, ordinary and enstatite) is −0.05±0.05‰ (2 S.E., n=11), with no significant differences existing between the different chondrites groups. In Eq. (3), $\delta^{57/54}Fe_{Sil}$, $\delta^{57/54}Fe_M$ and $\delta^{57/54}Fe_{FeS}$ are the Fe isotope compositions of the silicate, metal and sulphide fractions of the planet, respectively, and f_{Sil}, f_M and f_{FeS} are the corresponding proportions of the planets' Fe contents in these reservoirs, calculated from the mass fractions of the planet's mantle and cores and their Fe and S abundances. The values of $\delta^{57/54}Fe_{Sil}$ and $\delta^{57/54}Fe_{FeS}$ are related to that of $\delta^{57/54}Fe_M$ by the fractionation factors between metal and silicate ($\Delta^{57/54}Fe_{M\text{-}Sil}$) and metal and sulphide ($\Delta^{57/54}Fe_{M\text{-}FeS}$). Three sets of models with different values of $\Delta^{57/54}Fe_{M\text{-}Sil}$ were constructed. In the first group of models a value of 0.30‰ is used for $\Delta^{57/54}Fe_{M\text{-}Sil}$, based on the pallasite data of Zhu et al. [7], in a second set of models we use our value of $^{57/54}Fe_{M\text{-}Sil}$ (0.07‰) obtained from the IIE iron Watson, and, in a third set of models, no metal-silicate Fe isotope fractionation is allowed for ($\Delta^{57/54}Fe_{M\text{-}Sil}$=0‰). In all models $\Delta^{57/54}Fe_{M\text{-}FeS}$ is set at 0.79‰, the value obtained from North Chile, the only iron unambiguously in isotopic equilibrium. Using these fractionation factors, the values of $\delta^{57/54}Fe_M$, and hence those of $\delta^{57/54}Fe_{Sil}$ and $\delta^{57/54}Fe_{FeS}$, are determined from Eq. (1). In these models, cores contain 80 wt.% Fe and 1, 12 or 17 wt.% S, mantles contain 8 wt.% FeO and no S. Core S contents match the estimates of S in the initial cores of the parent bodies of the IVB, IIIAB and IIAB meteorites, respectively [32]. Core FeS contents are calculated by associating Fe with S on a 1:1 M basis, the remaining Fe is assumed to be metallic. Values of $\delta^{57/54}Fe_M$ determined for the three models are plotted against core mass fraction in Fig. 3.

All the models in Fig. 3 show that as the amount of S in the planet's core is increased, $\delta^{57/54}Fe_M$ increases. This is intuitive, as increasing the size of the FeS reservoir in a planet by increasing the core S content will increase the sink available for isotopically light Fe, driving the $\delta^{57/54}Fe$ values of the remaining reservoirs to heavier compositions. Increasing the core mass fraction of the planet intensifies this effect. Where $\Delta^{57/54}Fe_{M\text{-}Sil}$ is 0.30‰, $\delta^{57/54}Fe_M$ values are heaviest at low core mass fractions; the influence of core mass fraction being the most pronounced at low S contents (Fig. 3A). This is a consequence of light Fe being sequestered into the silicate part of the planet, in addition to the FeS component of the core. This effect decreases in importance with increasing core mass fraction and S content, as the FeS reservoir increases in size. At $\Delta^{57/54}Fe_{M\text{-}Sil}$=0.07‰ (Fig. 3B) the influence of the silicate reservoir is reduced and where $\Delta^{57/54}Fe_{M\text{-}Sil}$=0‰ (Fig. 3C), $\delta^{57/54}Fe_M$ (and $\delta^{57/54}Fe_{Sil}$)

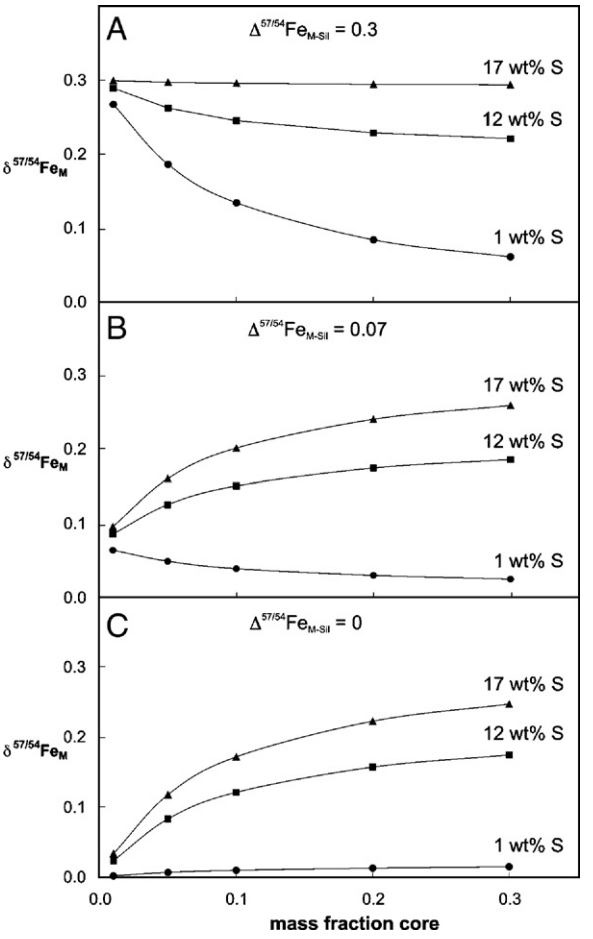

Fig. 3. Results of mass-balance calculations performed using Eq. (1), where the mass fraction of the planetary core is plotted against the corresponding isotopic composition of the metallic part of the core ($\delta^{57/54}Fe_M$). Each plot shows three separate model curves for different amounts of S (1, 12 and 17 wt.%) assumed to be in the cores of these planetesimals. For all models the metal–troilite fractionation factor ($\Delta^{57/54}Fe_{M\text{-}FeS}$) takes a constant value of 0.79‰. The metal-silicate fractionation factor ($\Delta^{57/54}Fe_{M\text{-}Sil}$) is 0.30, 0.07 and 0.0‰ in plots A), B) and C), respectively, where $\delta^{57/54}Fe_M$ is calculated for 1, 12 and 17 wt.% at a range of core mass fractions. No S is assumed to partition into the mantle.

increase with core mass fraction, with the effects being most pronounced at 17 wt.% S model and least at 1 wt.% S.

The relative differences in model $\delta^{57/54}Fe_M$ values can be compared to the average $\delta^{57/54}Fe$ values of the metal fractions of iron meteorites originating from parent bodies with different initial core S contents. Chabot et al. [32] recently proposed that the parental cores of the IIAB, IIIAB and IVB irons contained 17, 12 and ~1 wt.% S. Given the mass balance calculations described above, it is clear that the IIAB metals should be isotopically heavy with respect to the IIIAB and IVB metals, and that the latter should be the lightest,

assuming that they accreted with material having the same bulk $\delta^{57/54}$Fe value. This is in agreement with the observation that the weighted average $\delta^{57/54}$Fe value of the IIAB metals is 0.18±0.03‰, whereas the weighted average $\delta^{57/54}$Fe values of the IIIAB and IVB metals are 0.11±0.07‰ and 0.08±0.01‰, respectively, although the difference between the latter two could not be distinguished with the Students *t*-test, due to the small sample population. The IIAB and IVB metals show a difference in average $\delta^{57/54}$Fe values of 0.10‰. Assuming that the core mass fractions of the IIAB and IVB parent bodies were similar, this difference implies that their cores were relatively small, <8% of planet mass. This difference could also be produced if the core mass fractions of the IIAB and IVB parent bodies were very different. For example, in the case where $^{57/54}Fe_{M\text{-}Sil}$ is 0.07‰ and the core contains 17 wt.% S, the difference of 0.10‰ between the average $\delta^{57/54}$Fe values of the IIAB and IVB metals could be produced if the IIAB and IVB cores were 10% and 1% of the total planet mass, respectively. Given the difference in the S contents inferred for IIIAB and IVB cores, it is surprising that the average $\delta^{57/54}$Fe values of the IIIAB and IVB metals are so similar. However, this can be reconciled with our model if the cores of both parent bodies were 1–2% planet mass for all values of $\Delta^{57/54}Fe_{M\text{-}Sil}$.

4.4. Application of metal-sulphide fractionation to the terrestrial planets

Although recent studies of terrestrial basalts and peridotites [4,6] suggest that partial melts will be systematically heavier than their mantle protoliths by ~0.10‰, comparisons of terrestrial basalts with meteorites interpreted as the products of parent body mantle melting should still provide insights into the relative $\delta^{57/54}$Fe values of planetary mantles if this is taken into account. Terrestrial basalts, lunar rocks (excluding the High-Ti mare basalts, whose isotopic signatures may reflect derivation from an ilmenite-rich source region, c.f. [30]), martian meteorites, and meteorites believed to originate from the asteroid 4-Vesta have mean $\delta^{57/54}$Fe values of 0.11±0.04‰ (errors are given as 2 S.E.), 0.11±0.06‰, −0.02±0.04‰, and 0.03±0.04, respectively (for consistency values are all taken from [4]; these average values are in good agreement with [30]). There appears to be no difference between the average $\delta^{57/54}$Fe values of terrestrial and lunar mantle derived rocks if one excludes High-Ti mare basalts, but both averages are isotopically heavy relative to the average $\delta^{57/54}$Fe values of meteorites originating from Mars and 4-Vesta.

We can investigate whether or not these variations in mantle $\delta^{57/54}$Fe values originate from differences in the amount of S present in planetary cores using Eq. (3) and assuming that all planets accreted from bulk material with $\delta^{57/54}$Fe=0. The $\delta^{57/54}Fe_{Sil}$ values used in Eq. (3) are obtained by subtracting 0.10‰ from the average meteorite $\delta^{57/54}$Fe values determined for each parent body to allow for the systematic offset between mafic partial melts and their protoliths. The sizes of the FeS reservoirs, and hence the S contents of the different planetary cores, required to generate these $\delta^{57/54}Fe_{Sil}$ values are solved using Eq. (3) in conjunction with independent data on planetary core mass, core and mantle Fe contents [33–41]. Where $\Delta^{57/54}Fe_{M\text{-}Sil}$=0.30‰ and $\Delta^{57/54}Fe_{M\text{-}FeS}$=0.79‰, S contents calculated for the cores of the Earth and Moon range from 18 to 19 wt.% and from 17 to 22 wt.%, respectively, for appropriate core mass fractions, core and mantle Fe contents (Table 3). For Mars and 4-Vesta, core S contents are both 6.0 wt.%. These calculated S contents cannot be treated as real values as the bulk $\delta^{57/54}$Fe values of these planets are unknown, but the similarity of the core S contents inferred for Mars and 4-Vesta, planets that show extremely different levels of volatile element depletion [42,43], suggests that this model cannot be applied to large planets.

The model used above assumed that the three reservoirs of FeS, silicate and pure metal segregated and remained in equilibrium. A more realistic scenario may involve the initial segregation of metallic melt containing some S from a silicate melt, and subsequent segregation of an immiscible sulphide melt from a metallic melt in the cooling core. The actual amount of S in the initial metallic melt will be a function of the bulk planet S content. The second segregation event will not affect the isotopic composition of planetary mantles, so we can model the former process in terms of two reservoirs, assuming that all planets accreted from bulk material with the same $\delta^{57/54}$Fe value:

$$\delta^{57/54}Fe_B = \delta^{57/54}Fe_{\text{Mantle}} * f_{\text{Mantle}} + \delta^{57/54}Fe_{\text{Metal}} * f_{\text{Metal}} \quad (4)$$

In this model, we have to use an arbitrary fractionation factor between S rich metal and silicate melt as no applicable data exists for either natural samples or experiments. Using $\Delta^{57/54}Fe_{M\text{-}Sil}$ and $\Delta^{57/54}Fe_{M\text{-}FeS}$ values of 0.30‰ and 0.79‰, respectively, we calculate the fractionation factor between silicate and sulphide melts ($\Delta^{57/54}Fe_{Sil\text{-}FeS}$) to be 0.49‰. We calculate "weighted" fractionation factors between silicate and Fe-S melts ($\Delta^{57/54}Fe_{Mantle\text{–}Metal}$) assuming that FeS consists of Fe and S in 1:1 M abundance. For metallic melts

Table 3
Results of three-reservoir mass balance models

Planet	Mantle % planet mass	Core % planet mass	Core Fe (wt.%)	Mantle Fe (wt.%)	Bulk planet Fe (wt.%)	Mantle S (wt.%)	$\delta^{57/54}Fe_{Sil}$	$\Delta^{57/54}Fe_{M\text{-}Sil}$	$\Delta^{57/54}Fe_{M\text{-}FeS}$	Core S (wt.%)	Bulk planet S (wt.%)	Notes
Mars	78.30	21.70	77.80	13.99	27.84	0.00	−0.12	−0.30	−0.79	5.77	1.25	1)
	80.80	19.20	88.10	13.99	28.22	0.00	−0.12	″	″	6.39	1.23	2)
	77.00	23.00	76.30	13.76	28.14	0.00	−0.12	″	″	5.96	1.37	3)
Mars	78.30	21.70	77.80	13.99	27.84	0.00	−0.12	−0.07	−0.79	<0	<0	1)
	80.80	19.20	88.10	13.99	28.22	0.00	−0.12	″	″	<0	<0	2)
	77.00	23.00	76.30	13.76	28.14	0.00	−0.12	″	″	<0	<0	3)
Moon	99.00	1.00	70.63	8.68	9.30	0.00	0.01	−0.30	−0.79	22.15	0.22	4)
	98.00	2.00	70.63	8.77	10.00	0.00	0.01	″	″	19.03	0.38	4)
	97.00	3.00	70.63	8.86	10.71	0.00	0.01	″	″	17.99	0.54	4)
	96.00	4.00	70.63	8.95	11.42	0.00	0.01	″	″	17.47	0.70	4)
Moon	99.00	1.00	70.63	8.68	9.30	0.00	0.01	−0.07	−0.79	10.35	0.10	4)
	98.00	2.00	70.63	8.77	10.00	0.00	0.01	″	″	7.23	0.14	4)
	97.00	3.00	70.63	8.86	10.71	0.00	0.01	″	″	6.19	0.19	4)
	96.00	4.00	70.63	8.95	11.42	0.00	0.01	″	″	5.67	0.23	4)
Earth	67.50	32.50	85.00	6.38	31.93	0.25	0.01	−0.30	−0.79	19.24	6.42	5)
	67.50	32.50	80.00	6.22	30.20	0.25	0.01	″	″	18.12	6.06	6)
Earth	67.50	32.50	85.00	6.38	31.93	0.25	0.01	−0.07	−0.79	5.04	1.81	5)
	67.50	32.50	80.00	6.22	30.20	0.25	0.01	″	″	4.74	1.71	6)
4-Vesta	86.00	14.00	62.41	14.16	20.91	0.00	−0.07	−0.30	−0.79	6.01	0.84	7)
4-Vesta	86.00	14.00	62.41	14.16	20.91	0.00	−0.07	−0.07	−0.79	<0	<0	7)

Notes: Data for core:mantle mass fractions and iron contents from 1) Wänke and Dreibus 1994 [33]; 2) Gaetani and Grove, 1997 [34]; 3) Sanloup et al., 1999 model 2 [35]; 4) Iron contents of the lunar core and mantle derived from Logonne, 2003 [36], Righter, 2002 [37], Kuskov and Kronrod; 2001 [38] 5) Rubie et al., 2004 [39], and references therein; 6) McDonough, 1995 [40]; 7) Righter and Drake, 1997 [41], model of 0.3 CV chondrite: 0.7L chondrite source.

The results of mass balance models carried out using the three-reservoir model (Eq. (3)) in conjunction with average mantle $\delta^{57/54}$Fe values (obtained by subtracting 0.10‰ from the average $\delta^{57/54}$Fe values of mafic rocks and meteorites originating from each planetary body) and published constraints (see notes to Table and main text) on relative core and mantle mass fractions and iron contents. Model results are given in terms of both core and bulk planet S contents.

containing 15%, 10%, 5% and 2% S, $\Delta^{57/54}Fe_{Mantle-Metal}$ values are: −0.11‰, −0.17‰, −0.23‰, and −0.28‰, respectively using mantle and core Fe contents of 6 and 80 wt.%, respectively. Applying these $\Delta^{57/54}Fe_{Mantle-Metal}$ values to Eq. (4) produces a positive linear correlation between $\delta^{57/54}Fe_{Mantle}$ and $\Delta^{57/54}Fe_{Mantle-Metal}$ (Fig. 4A). In Fig. 4B, $\delta^{57/54}Fe_{Mantle}$ decreases with increasing core size, the effect being enhanced at the larger $\Delta^{57/54}Fe_{Mantle-Metal}$ value. As the size of the lunar core is inferred to be in the range of 1 to 4% planet mass [36] this model could explain why the Moon's mantle is isotopically heavy with respect to Mars and 4-Vesta. However, it does not explain why the Moon's mantle has the same $\delta^{57/54}$Fe value as that inferred for the Earth, nor can it explain why the Earth, which has a larger core than either Mars or 4-Vesta, has an isotopically heavier mantle. Therefore, the sequestering of isotopically light Fe into planetary cores is not a mechanism that can explain differences in planetary mantle $\delta^{57/54}$Fe values.

However, there are a number of specific processes inferred in the accretion history of the Earth that may potentially explain its heavy isotopic composition relative to Mars and 4-Vesta. These include events relating to the Moon-forming giant impact such as the mixing of the mantle and core of the impactor planet with the mantle and core of the proto-Earth [44] and the late segregation and "raining out" of an FeS melt from the silicate mantle of the proto-Earth to its core [45,46]. Alternatively, the heavy isotopic composition of the Earth with respect to Mars and 4-Vesta may be a function of the Earth's greater size and the stabilisation of perovskite within its mantle.

We can evaluate the first scenario, where the heavy mantle $\delta^{57/54}$Fe value of the Earth results from the admixing of impactor mantle material into the proto-Earth mantle, using a simple mixing model. We assume that the impactor planet, Theia, and the proto-Earth have the same core mass fractions (0.3), as would be expected if core formation is concurrent with accretion [47]. If Theia has 10 wt.% S in its core and 10 wt.% Fe in its mantle to concur with data from lunar rocks suggesting that the impactor was enriched in S and oxidised Fe [48], then the $\delta^{57/54}$Fe value of Theia's mantle is 0.10‰ heavier than that of the Earth, and the $\delta^{57/54}$Fe values of the cores of both the proto-Earth and Theia are the same. This calculation assumes that the proto-Earth's core

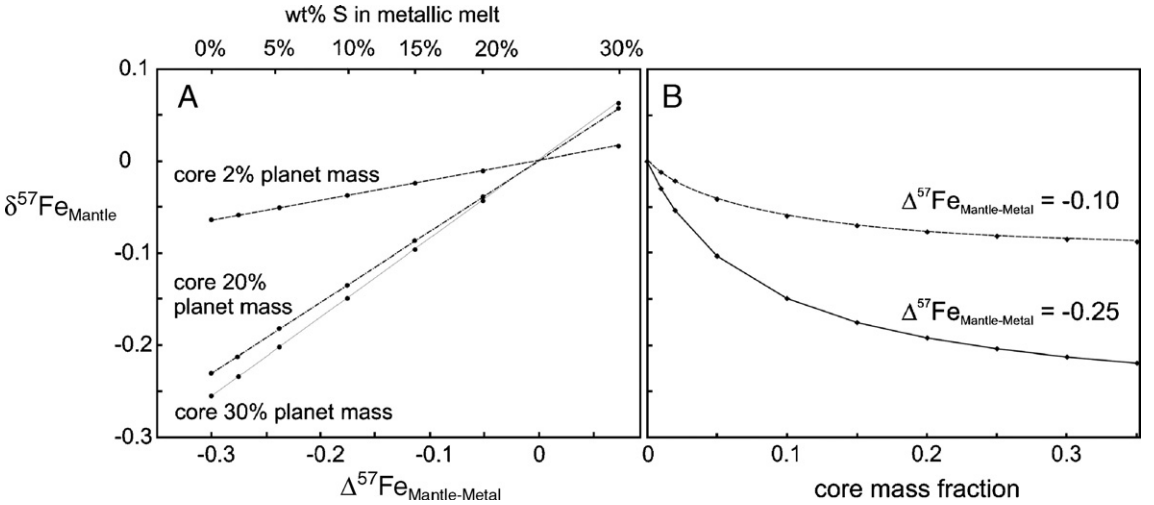

Fig. 4. Results of two reservoir mass balance calculations. A) $\delta^{57/54}Fe_{Mantle}$ values plotted against $\Delta^{57/54}Fe_{Mantle-Metal}$ values. $\Delta^{57/54}Fe_{Mantle-Metal}$ values are calculated from the $\Delta^{57/54}Fe_{M\text{-}Sil}$ and $\Delta^{57/54}Fe_{Sil\text{-}FeS}$ values obtained from iron meteorites and are weighted according to the amounts of S present in the metallic melts (see main text for details), which are shown on the upper *x*-axis of Fig. 4A. B) $\delta^{57/54}Fe_{Mantle}$ values plotted against core mass fraction for two different $\Delta^{57/54}Fe_{Mantle-Metal}$ values, −0.10‰ and −0.25‰, which correspond to metal S contents of 16.1 and 4.0 wt.%, respectively.

contains 1 wt.% S and its mantle 6 wt.% Fe, allowing for a proto-Earth core S content of 2% shifts the $\delta^{57/54}$Fe value of the proto-Earth's mantle by only 0.01‰. If the Fe content of Theia's mantle is reduced to 6 wt.%, the isotopic compositions of its core and mantle only changes by 0.01‰. In order to increase the $\delta^{57/54}$Fe value of the Earth's mantle by at least 0.08‰ (the difference between the average mantle $\delta^{57/54}$Fe values of the Earth and 4-Vesta) a contribution of 70% impactor mantle to the Earth's mantle is required, which is unrealistic. No amount of impactor mantle contribution can increase the $\delta^{57/54}$Fe value of the Earth's mantle by 0.13‰ (the difference between the average mantle $\delta^{57/54}$Fe values of the Earth and Mars).

Late removal of ~0.5% sulphide melt from the proto-Earth mantle to the core following the giant impact has been proposed as a means of reconciling the different timescales for core segregation required by Hf–W and U–Pb data [45,46]. Using the value of 0.49‰ derived earlier for $\Delta^{57/54}Fe_{Sil\text{-}FeS}$ and assuming the sulphide melt consists of Fe and S in a 1:1 M ratio, we calculate that removing 0.5% sulphide melt from the proto-Earth's mantle will only increase the latter's $\delta^{57/54}$Fe value by 0.03‰. Increasing the amount of sulphide melt removal to 1% raises the $\delta^{57/54}$Fe value of the proto-Earth's mantle by 0.06‰. Both of the isotopic shifts calculated fall far short of the increase in $\delta^{57/54}$Fe value of the Earth's mantle needed to explain the different $\delta^{57/54}$Fe values of the mantles of the Earth, 4-Vesta and Mars.

The oxidised nature of the Earth's mantle is at odds with the reduced conditions required from the partitioning of elements such as silicon and tungsten into the Earth's core, and it has been proposed that the core segregated under initially reducing conditions and that the Earth's mantle became oxidised in the final phases of accretion. One mechanism for oxidising the Earth's mantle is the disproportionation of Fe^{2+} to Fe^{3+} and Fe^0 by magnesium silicate perovskite [45]:

$$\begin{aligned} &3FeO + Al_2O_3 \leftrightarrow 2FeAlO_3 + Fe^0 \\ &(\text{Silicate melt}) \leftrightarrow (\text{perovskite} + \text{metal}) \end{aligned} \quad (5)$$

Although there are no experimental data for Fe isotope fractionation between these phases, theoretical studies suggest that phases enriched in Fe^{3+} will be isotopically heavy relative to native Fe, and that phases where Fe^{2+} predominates will be isotopically lighter [9]. Therefore the disproportionation of FeO present in the proto-Earth mantle could result in perovskite with a heavy Fe isotope composition, and isotopically light metallic Fe. Segregation of the metal into the core and the release of the Fe^{3+} hosted in perovskite into the magma ocean would drive the reaction above to the right, and increase the $\delta^{57/54}$Fe value of the Earth's mantle. While this mechanism must remain speculative in the present absence of experimental data for isotopic fractionation between these phases, it does provide a good explanation for the heavy $\delta^{57/54}$Fe value of the Earth's mantle relative to that of Mars and 4-Vesta. Mars and 4-Vesta are both small planets, where the pressures required to stabilise significant amounts of perovskite in the mantle (>23 GPa) were not reached, precluding

perovskite-induced disproportionation of FeO. This mechanism can also explain the similarity in the $\delta^{57/54}$Fe values of the Moon's mantle to that of the Earth's. If, as is widely believed, the Moon's mantle is largely derived from the impacting planet, Theia, then the isotopically heavy signature of the Moon's mantle requires that Theia also had a mantle with a $\delta^{57/54}$Fe value heavier than that of Mars or 4-Vesta. This would imply that Theia's mantle must have been rendered isotopically heavy by perovskite-induced disproportionation of Fe during accretion, requiring that Theia was larger than Mars.

Acknowledgements

The authors would like to thank M. Drake, S. P. Kelley, S. Nielsen, F. Poitrasson, M. Rehkämper, R. Wieler and E. Schauble for their helpful discussions. The first author is extremely grateful to E. Schauble for his explanations of the theoretical aspects of stable isotope fractionation, and to J. Schuessler and J. Yang for generously sharing their unpublished data and manuscripts. S. Nielsen and S. Woodland are acknowledged for their contributions of dissolved sample aliquots. C. Stirling, U. Menet and F. Oberli are thanked for their technical help. The authors would like to raise their glasses to T. Elliott for his thoughtful and constructive review. S. King is thanked for his help and patience. This work was funded by the Swiss National Science Foundation.

References

[1] J.T. Wasson, G.W. Kallemeyn, The IAB iron–meteorite complex: a group, five subgroups, numerous grouplets, closely related, mainly formed by crystal segregation in rapidly cooling melts, Geochim. Cosmochim. Acta 66 (2002) 2445–2473.

[2] J.T. Wasson, Trapped melt in IIIAB irons; solid/liquid elemental partitioning during the fractionation of the IIIAB magma, Geochim. Cosmochim. Acta 63 (1999) 2875–2889.

[3] B.L. Beard, C.M. Johnson, Inter-mineral Fe isotope variations in mantle-derived rocks and implications for the Fe geochemical cycle, Geochim. Cosmochim. Acta 68 (2004) 4727–4743.

[4] S. Weyer, A.D. Anbar, G.P. Brey, C. Munker, K. Mezger, A.B. Woodland, Iron isotope fractionation during planetary differentiation, Earth Planet. Sci. Lett. 240 (2005) 251–264.

[5] H.M. Williams, C.A. McCammon, A.H. Peslier, A.N. Halliday, N. Teutsch, S. Levasseur, J.P. Burg, Iron isotope fractionation and the oxygen fugacity of the mantle, Science 304 (2004) 1656–1659.

[6] H.M. Williams, A.H. Peslier, C. McCammon, A.N. Halliday, S. Levasseur, N. Teutsch, J.-P. Burg, Systematic iron isotope variations in mantle rocks and minerals: the effects of partial melting and oxygen fugacity, Earth Planet. Sci. Lett. 235 (2005) 435–452.

[7] X.K. Zhu, Y. Guo, R.J.P. Williams, R.K. O'Nions, A. Matthews, N.S. Belshaw, G.W. Canters, E.C. de Waal, U. Weser, B.K. Burgess, B. Salvato, Mass fractionation processes of transition metal isotopes, Earth Planet. Sci. Lett. 200 (2002) 47–62.

[8] F. Poitrasson, S. Levasseur, N. Teutsch, Significance of iron isotope mineral fractionation in pallasites and iron meteorites for the core–mantle differentiation of terrestrial planets, Earth Planet. Sci. Lett. 234 (2005) 151–164.

[9] V.B. Polyakov, S.D. Mineev, The use of Mössbauer spectroscopy in stable isotope geochemistry, Geochim. Cosmochim. Acta 64 (2000) 849–865.

[10] E.A. Schauble, G.R. Rossman, H.P. Taylor Jr., Theoretical estimates of equilibrium Fe-isotope fractionation from vibrational spectroscopy, Geochim. Cosmochim. Acta 65 (2001) 2487–2497.

[11] A. Markowski, G. Quitté, A.N. Halliday, T. Kleine, Tungsten isotopic compositions of iron meteorites: chronological constraints vs. cosmogenic effects, Earth Planet. Sci. Lett. 242 (2006) 1–15.

[12] S.G. Nielsen, M. Rehkämper, A.N. Halliday, Large thallium isotopic variations in iron meteorites and evidence for lead-205 in the early solar system, Geochim. Cosmochim. Acta 70 (2006) 2643–2657.

[13] S.J. Woodland, M. Rehkämper, A.N. Halliday, D.-C. Lee, B. Hattendorf, D. Gunther, Accurate measurement of silver isotopic compositions in geological materials including low Pd/Ag meteorites, Geochim. Cosmochim. Acta 69 (2005) 2153–2163.

[14] G. Quitté, M. Meier, C. Latkoczy, A.N. Halliday, D. Gunther, Nickel isotopes in iron meteorites-nucleosynthetic anomalies in sulphides with no effects in metals and no trace of ^{60}Fe, Earth Planet. Sci. Lett. 242 (2006) 16–25.

[15] J. Koblitz, METBASE: Meteorite Data Retrieval Program, Fischerhude, Germany, 2003.

[16] R. Brett, P.M. Bell, Melting relations in the Fe-rich portion of the system Fe–FeS at 30 kb pressure, Earth Planet. Sci. Lett. 6 (1969) 479–482.

[17] D.C. Dean, J.I. Goldstein, Determination of the interdiffusion coeficients in the Fe–Ni and Fe–Ni–P systems below 90 °C, Metall. Trans., A, Phys. Metall. Mater. Sci. 17A (1986) 1131–1138.

[18] A. Tsuchiyama, K. Kawamura, T. Nakao, C. Uyeda, Isotopic effects on diffusion in MgO melt simulated by the molecular dynamics (MD) method and implications for isotopic mass fractionation in magmatic systems, Geochim. Cosmochim. Acta 58 (1994) 3013–3021.

[19] F.M. Richter, A.M. Davis, D.J. DePaolo, E.B. Watson, Isotope fractionation by chemical diffusion between molten basalt and rhyolite, Geochim. Cosmochim. Acta 67 (2003) 3905–3923.

[20] M. Roskosz, B. Luais, H.C. Watson, M.J. Toplis, C.M.O.D. Alexander, B.O. Mysen, Experimental quantification of the fractionation of Fe isotopes during metal segregation from a silicate melt, Earth Planet. Sci. Lett. 248 (2006) 851–867.

[21] G. Quitté, B. Bourdon, H.M. Williams, A.N. Halliday, Kinetic isotopic fractionation of nickel in iron meteorites, Earth Planet. Sci. Lett. (submitted for publication).

[22] J. Schuessler, R. Schoenberg, H. Behrens, F. von Blanckenburg, Experimental calibration of the Fe isotope fractionation factor between pyrrhotite and silicate melt, Geochim. Cosmochim. Acta 69 (2005) A211.

[23] J. Schuessler, R. Schoenberg, H. Behrens, F. von Blanckenburg, Experimental evidence for high temperature iron isotope fractionation factor between pyrrhotite and peralkaline rhyolitic melt, Geochim. Cosmochim. Acta (submitted for publication).

[24] R.H. Condit, R.R. Hobbins, C.E. Birchenall, Self-diffusion of iron and sulfur in ferrous sulfide, Oxid. Met. 8 (1974) 409–455.

[25] E. Randich, J.I. Goldstein, Cooling rates of seven hexahedrites, Geochim. Cosmochim. Acta 42 (1978) 221–233.

[26] V.F. Buchwald, Handbook of Iron Meteorites, Their History, Distribution, Composition and Structure, University of California, Los Angeles, 1975 1418 pp.

[27] J. Yang, J.I. Goldstein, Metallographic cooling rates of the IIIAB iron meteorites, Geochim. Cosmochim. Acta 70 (2006) 3197–3215.
[28] K.L. Rasmussen, F. Ulff-Moller, H. Haack, The thermal evolution of IVA iron meteorites: evidence from metallographic cooling rates, Geochim. Cosmochim. Acta 59 (1995) 3049–3059.
[29] K. Kehm, E.H. Hauri, C.M.O. Alexander, R.W. Carlson, High precision iron isotope measurements of meteoritic material by cold plasma ICP-MS, Geochim. Cosmochim. Acta 67 (2003) 2879–2891.
[30] F. Poitrasson, A.N. Halliday, D.-C. Lee, S. Levasseur, N. Teutsch, Iron isotope differences between Earth, Moon, Mars and Vesta as possible records of contrasted accretion mechanisms, Earth Planet. Sci. Lett. 223 (2004) 253–266.
[31] X.K. Zhu, Y. Guo, R.K. O'Nions, E.D. Young, R.D. Ash, Isotopic homogeneity of iron in the early solar nebula, Nature 412 (2001) 311–313.
[32] N.L. Chabot, Sulfur contents of the parental metallic cores of magmatic iron meteorites, Geochim. Cosmochim. Acta 68 (2004) 3607–3618.
[33] H. Wänke, G. Dreibus, Chemistry and accretion history of Mars, Philos. Trans. R. Soc. Lond. Ser. A: Math. Phys. Sci. 349 (1994) 285–293.
[34] G.A. Gaetani, T.L. Grove, Partitioning of moderately siderophile elements among olivine, silicate melt, and sulfide melt: constraints on core formation in the Earth and Mars, Geochim. Cosmochim. Acta 61 (1997) 1829–1846.
[35] C. Sanloup, A. Jambon, P. Gillet, A simple chondritic model of Mars, Phys. Earth Planet. Inter. 112 (1999) 43–54.
[36] P. Lognonne, J. Gagnepain-Beyneix, H. Chenet, A new seismic model of the Moon: implications for structure, thermal evolution and formation of the Moon, Earth Planet. Sci. Lett. 211 (2003) 27–44.
[37] K. Righter, Does the Moon have a metallic core? Constraints from giant impact modeling and siderophile elements, Icarus 158 (2002) 1–13.
[38] O.L. Kuskov, V.A. Kronrod, Core sizes and internal structure of Earth's and Jupiter's satellites, Icarus 151 (2001) 204–227.
[39] D.C. Rubie, C.K. Gessmann, D.J. Frost, Partitioning of oxygen during core formation on the Earth and Mars, Nature 429 (2004) 58–61.
[40] W.F. McDonough, S.S.-s. Sun, The composition of the Earth, Chem. Geol. 120 (1995) 223–253.
[41] K. Righter, M.J. Drake, Formation of eucrites and diogenites by equilibrium crystallization of a chondritic magma ocean, Meteorit. Planet. Sci. 32 (1997) A109–A110.
[42] G. Dreibus, H. Palme, Cosmochemical constraints on the sulfur content in the Earth's core, Geochim. Cosmochim. Acta 60 (1996) 1125–1130.
[43] A.N. Halliday, D. Porcelli, In search of lost planets — the paleocosmochemistry of the inner solar system, Earth Planet. Sci. Lett. 192 (2001) 545–559.
[44] A.G.W. Cameron, From interstellar gas to the Earth–Moon system, Meteorit. Planet. Sci. 36 (2001) 9–22.
[45] B.J. Wood, A.N. Halliday, Cooling of the Earth and core formation after the giant impact, Nature 437 (2005) 1345–1348.
[46] B.J. Wood, M.J. Walter, J. Wade, Accretion of the Earth and segregation of its core, Nature 441 (2006) 825–833.
[47] A.N. Halliday, Mixing, volatile loss and compositional change during impact-driven accretion of the Earth, Nature 427 (2004) 505–509.
[48] H.G. Jones, H. Palme, Geochemical constraints on the origin of the Earth and Moon, in: R. Canup, K. Righter (Eds.), Origin of the Earth and Moon, University of Arizona Space Science Series, University of Arizona Press, Tucson, 2000, pp. 197–216.